Available online at www.sciencedirect.com
SCIENCE DIRECT
International Journal of Heat and Mass Transfer 49 (2006) 2771–2780
International Journal of HEAT and MASS TRANSFER
www.elsevier.com/locate/ijhmt

Dynamics of boiling succeeding spontaneous nucleation on a rapidly heated small surface

Kunito Okuyama *, Shoji Mori, Kimihiro Sawa, Yoshihiro Iida

Department of Chemical Engineering Science, Yokohama National University, 79-5 Tokiwadai, Hodogaya-ku, Yokohama 240-8501, Japan

Received 13 June 2005; received in revised form 14 November 2005
Available online 24 February 2006

Abstract

The dynamics of boiling succeeding spontaneous nucleation on a small film heater immersed in ethyl alcohol are investigated at heating rates ranging from 10^7 K/s to approximately 10^9 K/s, under which spontaneous nucleation is dominant for the inception of boiling. Immediately after the concurrent generation of a large number of fine bubbles, a vapor film that covers the entire surface is formed by coalescence and rapidly expands to a single bubble. As the heating rate is increased, the coalesced bubble flattens and only a thin vapor film grows before cavitation collapse. Similar behaviors are also observed for water. Based on the observed results, a theoretical model of the dynamic bubble growth due to the self-evaporation of the superheated liquid layer, which develops before boiling incipience, is presented. The calculated results are compared with the observed results.

Keywords: Bubble dynamics; Spontaneous nucleation; Small film heater; Rapid heating

1. Introduction

When a solid immersed in a liquid is heated at a very high rate, spontaneous nucleation, as a result of random fluctuations of the molecular energy of the liquid, may occur on the surface of the solid at a temperature close to the limit of liquid superheat. The rapid boiling phenomena initiated under such conditions are quite different from those of steady-state boiling and are receiving a great deal of attention for applications such as flashing, vapor explosions and the drive mechanism in thermal ink jet (TIJ) printers. Boiling dynamics and the related heat transfer succeeding spontaneous nucleation, particularly on a small surface, are important with respect to application to microactuators that utilize rapid phase change phenomena.

Iida et al. investigated the nucleation phenomenon by realizing high-rate heating of up to 9.3×10^7 K/s as well as simultaneous surface temperature measurement using a small platinum film heater having a heating area of 100 μm × 400 μm [1–3]. The heater temperature at boiling incipience was saturated at approximately 1.0×10^7 K/s for ethyl alcohol and toluene (at approximately 4.5×10^7 K/s for water) and, for ethyl alcohol, this value agreed with the homogeneous nucleation temperature. A number of tiny bubbles of uniform size were generated immediately after boiling incipience, and the number of bubbles tended to increase as predicted by the homogeneous nucleation theory. Based on the experimental results, the dominant mechanism of the peculiar bubble generation was concluded to be spontaneous nucleation. The process of boiling succeeding spontaneous nucleation and the corresponding heat transfer were also studied using the same heater for ethyl alcohol by changing the system pressure and liquid temperature [4,5]. No appreciable increase in the heat transfer rate was measured despite the concurrent generation of a tremendous number of fine bubbles. These bubbles immediately coalesced with each other to form a vapor film covering the entire heater surface, which led to a marked decrease in heat transfer. After the rapid expansion of the vapor film into a single bubble, the bubble

* Corresponding author. Tel./fax: +81 45 339 4009.
E-mail address: okuyama@ynu.ac.jp (K. Okuyama).

0017-9310/$ - see front matter © 2006 Elsevier Ltd. All rights reserved.
doi:10.1016/j.ijheatmasstransfer.2006.01.002

Nomenclature

A_l	inertance of liquid [kg/m^4]
$\overline{B}$	average rate of temperature increase [K/s]
c_p	specific heat [J/(kg K)]
d_h	length of one side of the square heater [m]
H_{fg}	latent heat of vaporization [J/kg]
P	system pressure [MPa]
P_v	pressure in vapor film [MPa]
P_∞	ambient pressure [MPa]
Q	heat generation rate per unit surface area [W/m^2]
q_f	heat flux transferred to fluid [W/m^2]
q_i	heat flux at liquid–vapor interface [W/m^2]
q_{lBI}	heat flux transferred to liquid at boiling incipience [W/m^2]
q_{qg}	heat flux transferred to quartz glass [W/m^2]
S_h	heater surface area [m^2]
T_{wBI}	heater surface temperature at boiling incipience [°C]
T_i	temperature at liquid–vapor interface [°C]
T_{l0}	liquid bulk temperature [°C]
T_{sat}	saturation temperature [°C]
t	time elapsed after onset of heating [μs]
t_g	time elapsed after onset of growth of vapor film [μs]
V_v	volume of vapor film on the heater [m^3]
δ	film thickness [m]
κ	thermal diffusivity [m^2/s]
λ	thermal conductivity [W/(mK)]
ρ	density [kg/m^3]
τ_h	pulse heating period [s]
τ_g	bubble growth period [s]

Subscripts

Cr	chromium
l	liquid
Pt	platinum
v	vapor
0	initial state

shrank, followed by a marked increase in heat transfer at the collapse. The time variation of the bubble size up to the collapse was dominated by the heating rate from the onset of heating to the coalescence, regardless of the continuation of heating after the coalescence. The lifetime of the bubble became significantly shorter with the increase in the system pressure and the decrease in the liquid bulk temperature. Similar behaviors were also observed for water.

Asai et al. investigated the boiling of a water-based ink and of methyl alcohol occurring on small film heaters (with a heating area on the order of 100 μm × 100 μm) under high heat flux pulse heating (from 5 to 50 MW/m^2 for methyl alcohol) [6,7]. Asai also presented an analytical model for the bubble generation due to spontaneous nucleation followed by instantaneous formation of a vapor film, rapid bubble growth and cavitation bubble collapse [7]. It was assumed that the vapor pressure impulse arising immediately after vapor film formation supplies the initial momentum for the liquid surrounding the vapor film, and thereafter the bubble growth and collapse are dynamically controlled by the pressure difference and the liquid inertia. The maximum volume and the lifetime of the bubble were correlated analytically with the magnitude of the pressure impulse for a prescribed film heater size.

Ueno et al. investigated the nucleation and pressure generation on a solid silicon surface irradiated in water by a high-power nanosecond Nd:YAG laser pulse [8]. Formation of bubbles having a radius on the order of 80 nm was detected approximately 10–20 ns after the onset of irradiation from the reflectance signal of a probing He–Ne laser. A shockwave on the order of 1 MPa was generated. The period from heating onset to bubble formation was compared with the time required for the solid surface to reach the homogeneous nucleation temperature via heat conduction. A one-dimensional theoretical model of the pressure generation accompanying the shock wave propagation due to the rapid evaporation was proposed, and the predictions agreed well with the experimental results.

Extensive review has been given in literature for the researches related to spontaneous nucleation and the consequent explosive vaporization on the microscopic level on a solid surface subjected to high pulse heating [9,10].

The present paper focuses on the variation of the dynamics of the coalesced bubble succeeding the spontaneous nucleation on a small film heater for an extremely high heating rate. The bubble behavior at an extremely high rate of heating may provide useful information for predicting phenomena that occur under direct contact heating, in which the surface temperature increases ideally at an infinite rate. The heating rate is widely varied up to approximately two orders of magnitude larger than the minimum rate (approximately 1.0×10^7 K/s for ethyl alcohol) required for realizing spontaneous nucleation, and its effects on the formation, growth and collapse processes of the coalesced bubble are investigated. Based on the observed results, a theoretical model for the dynamic bubble growth due to self-evaporation of the superheated liquid layer, which develops on the heater surface until the boiling incipience, and the subsequent collapse is presented. The theoretically calculated results are compared with the observed results.

2. Experimental apparatus and procedure

The test specimen and the experimental apparatus are fundamentally the same as those used by the authors in previous experiments examining spontaneous nucleation [1–3]. The heating circuit was improved so that the platinum film can be heated at a much higher rate in the test liquid without losing the temperature measurement accuracy.

Fig. 1 shows a sketch of the test film heater. The small film heater, which has a thickness of 0.25 μm, was made by sputtering chromium and platinum onto a quartz glass substrate. The film heater has a 0.10-mm-wide heating section and two voltage taps separated by 0.25 mm. The film heater was exposed once to a 150 °C de-oxidized atmosphere for 1 h and then to a 500 °C de-oxidized atmosphere for 2 h before the boiling experiment so that the temperature-resistance relationship of the film would be stabilized. The heater surface was cleaned with trichloroethylene prior to setup. The heater was immersed in a glass cell filled with degassed (boiled for 2 h) test liquid (ethyl alcohol and water of reagent grade) with its surface upward. The liquid surface, which was separated from the heater by a distance of 5 mm, was covered with a glass cover slide to make the surface flat. The experiment was conducted at atmospheric pressure and a liquid bulk temperature of 25 °C.

Fig. 2 shows a schematic diagram of the experimental apparatus. A square wave voltage signal was amplified by a power amplifier and the heating current was supplied pulsewise to the film heater. The voltage difference between two voltage taps and the heating current were recorded using a digital oscilloscope via a differential amplifier and a current probe, respectively, and were then transmitted to a personal computer. The average temperature of the film heater was obtained by referencing the measured electrical resistance to the temperature-resistance calibration curve, which was carefully obtained in the temperature range of interest using a thermostatic bath. The error in the measurement of the average temperature of the film in contact with test liquid was estimated to be within ±5 K. The heat flux q_f transferred to the fluid was obtained by subtracting the conduction heat flux q_{qg} transferred to the quartz substrate and the heat storage rate in the heater film from the heat generation rate per unit surface area of the heater Q, according to the following equation:

$$q_f(t) = Q(t) - q_{qg}(t) - \left\{(c_p\rho\delta)_{Pt} + (c_p\rho\delta)_{Cr}\right\}\frac{dT_w}{dt} \quad (1)$$

The value of q_{qg} was calculated from the numerical solution of the one-dimensional transient heat conduction equation for a semi-infinite medium (quartz glass). The time sequence of the film temperature measured was used as one of the boundary conditions, and the temperature dependency of the thermophysical properties was taken into account in the calculation. The time-averaged value of the wall heat flux to the liquid from onset of heating to boiling incipience was estimated to be approximately 25% of the heating power per unit heating area for ethyl alcohol and approximately 52% for distilled water.

The behavior of the boiling bubbles was observed through a microscope at 50× magnification and photographed using a 35 mm camera and a 10 ns pulse stroboscopic light. The timing of the lighting was controlled by a delay unit triggered by the onset of heating. One flash per picture frame enabled confirmation as to whether the boiling phenomena were reproducible for further pulses under the same heating conditions. The time-sequence from bubble generation to collapse was recorded by changing the timing of the lighting. The ISO 3200 film used for photography was sensitized so as to be equivalent to ISO 20000.

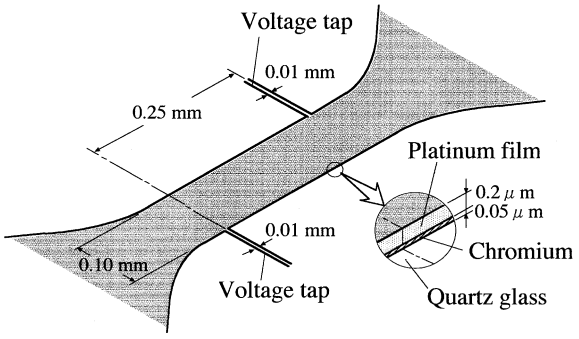

Fig. 1. Sketch of test film heater.

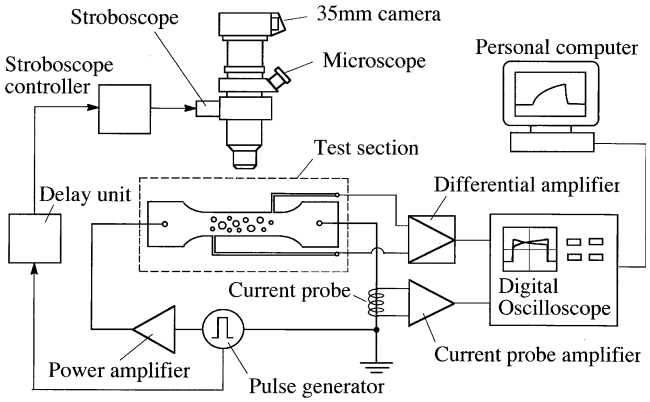

Fig. 2. Schematic diagram of the experimental apparatus.

3. Experimental results and discussion

Fig. 3 shows the heater temperature at boiling incipience of ethyl alcohol T_{wBI} plotted with respect to the average rate $\overline{B}$ of the wall temperature increase from onset of heating to boiling incipience. In the present observation system, boiling incipience was defined as the time at which the initial bubble was captured. The solid line represents the theoretical temperature of homogeneous nucleation, which increases slightly with the rate of temperature increase. The theoretical value was obtained by employing the expression of the nucleation rate presented by Volmer [11,12] and

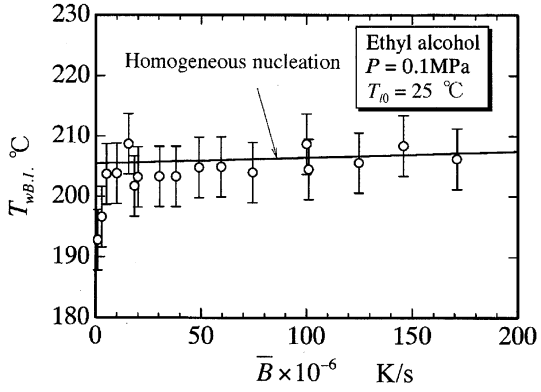

Fig. 3. Heater temperature at boiling incipience plotted with respect to average rate of wall temperature increase from heating onset to boiling incipience (ethyl alcohol).

integrating the value numerically over the superheated liquid layer and with time until one bubble is counted on the heater area. The measured temperature at boiling incipience was confirmed to be saturated at the rates of wall temperature increase higher than approximately 1.0×10^7 K/s and to agree with the theoretical value within the estimated error even at the rates up to 1.7×10^8 K/s, which was the maximum rate that the heater temperature can be measured without losing the accuracy using the current measurement system.

Fig. 4 shows the boiling photographs of ethyl alcohol at the heating rate slightly larger than the minimum (approximately 1.0×10^7 K/s) in the rate range that the temperature at boiling incipience agrees with the homogeneous nucleation temperature. Here, q_{lBI} is the heat flux transferred to liquid at boiling incipience and equal to the value of q_{f} at the time of boiling incipience in Eq. (1). τ_{h} is the pulse heating period. Side views of the bubbles are also shown in Fig. 4(a), in which the boiling stage in each frame corresponds approximately to that of the top view. Fig. 4(b) shows magnified top views of boiling bubbles immediately after boiling incipience. A thin vapor film is formed by the immediate coalescence of a large number of fine nucleated bubbles of less than 1 μm in diameter. The film, which is of almost uniform thickness (frames ④ and ④′ in Fig. 4(a) and frame ④ in Fig. 4(b)), grows into a single bubble with time (frames ⑤ and ⑤′) and then shrinks from the side before collapsing in the center of the heater (frames ⑦ and ⑦′). The maximum height of the bubble is approximately 50 μm. Significant re-growth is also observed after the collapse (frame ⑧ and ⑧′). The re-growth may be due to the depressurization at the rebound of liquid after the collision to the heater surface. The thickness of the microlayer formed beneath the nucleated bubbles observed in Fig. 4(b) can be estimated to be less than 0.1 μm according to the theory of the microlayer formation based on hydrodynamics derived by Cooper and Lloyd [13], which is much smaller than the thickness of the superheated liquid layer to be developed before the boiling incipience (approximately 0.8 μm).

Fig. 5 shows top-view photographs of ethyl alcohol boiling at higher heating rates. The heating rate in Fig. 5(a) is approximately 12 times higher than that in Fig. 4(a). At such a high heating rate, the accuracy in the heater temperature measurement was considerably lower as a result of the effect of the reactance in the circuit. The heating rate $\overline{B}$, therefore, was estimated by assuming that the heater temperature at the time at which the initial bubble is detected will be equal to the homogeneous nucleation temperature. The heat flux q_{lBI} was also calculated by extrapolating the relationship at the lower heating rates between the rate of temperature increase and the heat flux. These approximated values of $\overline{B}$ and q_{lBI} are denoted by parentheses ()*. Bubbles initially appear on the side edge of the heater (frame ① in Fig. 5(a)). Approximately 0.1 μs later, a tremendous number of fine bubbles are concurrently generated by spontaneous nucleation on the entire heater surface (frame ②). These bubbles immediately coalesce with each other, forming a thin vapor film that covers the heater (frame ③). The vapor film does not appear to grow to appreciable thickness, compared to those generated at lower heating rates (for example, frame ⑤ in Fig. 4(a)), but rather remains thin, even during the shrinking phase before collapse (frames ⑤ to ⑧ in Fig. 5(a)). The bubble lifetime from boiling incipience to collapse becomes short, approximately 40% of that shown in Fig. 4(a). Precisely measuring the maximum vapor film thickness from the side is difficult, but the film thickness may be assumed, based on top-view observation, to be approximately on the order of several micrometers in the central region of the heater, which is less than 10% of the maximum bubble height shown in Fig. 4(a). The significant decrease in the vapor film thickness at higher heating rates is similar to that observed for the TIJ heater [14]. Thicker vapor film regions can be found around both heater ends and the bases of the voltage taps of the platinum film heater. The current density around the end region of the heater must be lower than that in the central region because of the enlarged width of the structure. In addition, the fin cooling action around the tap bases along the platinum film may be significant. These effects locally reduce the heating rate, which may result in a slight delay in reaching the spontaneous nucleation temperature and greater superheat energy storage before the nucleation. The heating rate shown in Fig. 5(b) is approximately three times larger than that shown in Fig. 5(a). Distinguishing each nucleated bubble is difficult due to their marked increase and immediate coalescence, a phenomenon which appears as if a very thin vapor film gushes out uniformly from the entire heated surface (frames ① to ④ in Fig. 5(b)). Even at maximum thickness (frames ⑥ in Fig. 5(b)), the film thickness appears to be less than that in Fig. 5(a) (frames ⑥).

Fig. 6 shows boiling photographs of water at two high heating rates of over 10^8 K/s. The accuracy in the heater temperature measurement was also lost similarly to the cases of ethyl alcohol shown in Fig. 5. In the previous study by the authors [2], it was shown that the heater temperature

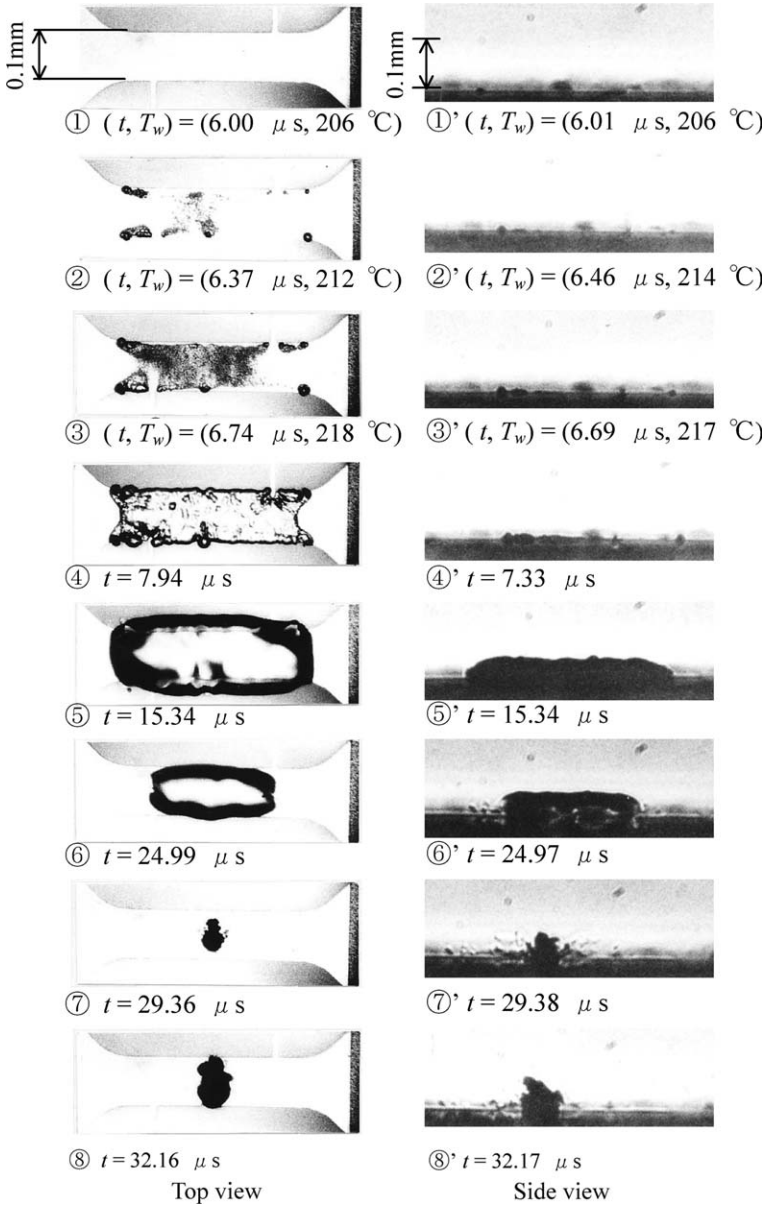

Fig. 4(a). Top and side views of boiling bubbles after boiling incipience on the film heater subjected to high pulse heating (ethyl alcohol, $P = 0.1$ MPa, $T_{l0} = 25$ °C) $\overline{B} = 3.0 \times 10^7$ K/s, $q_{IBI} = 35$ MW/m^2, $\tau_h = 7.6$ μs.

at boiling incipience of water was saturated at approximately 4.5×10^7 K/s and this value remained at 296 °C, which is approximately 19 K lower than the homogeneous nucleation temperature, up to 9.3×10^7 K/s. The heating rate $\overline{B}$, therefore, was estimated by assuming that the heater temperature at boiling incipience will be still 296 °C in Fig. 6. The boiling bubble behavior and the tendency of its change with respect to the increase in the heating rate are similar to those for ethyl alcohol shown in Fig. 5.

The results shown in Figs. 5 and 6 suggest that vapor production becomes negligibly small at an infinitely large rate of surface temperature increase, which is assumed to be the case for direct contact between hot and cold surfaces separated beforehand. It seems that there is a contradiction for understanding the mechanism of the explosive evaporation in vapor explosion. However, the pressure impulse generated by the rapid phase-change near the superheat limit may cause intensive interaction between liquids. Furthermore, in the present system, a heat source exists on the interface between the liquid and the solid, which differs from liquid–liquid contact system. We cannot directly discuss the thermal-fluid interaction in the liquid–liquid system based only on the current results.

Based on a previous study, the present authors concluded [5] that the growth of the coalesced bubble may be due primarily to the self-evaporation of the superheated liquid layer that developed before boiling incipience. The superheat energy at boiling incipience decreases with the increase in the heating rate, because boiling is always initiated at around the homogeneous nucleation temperature,

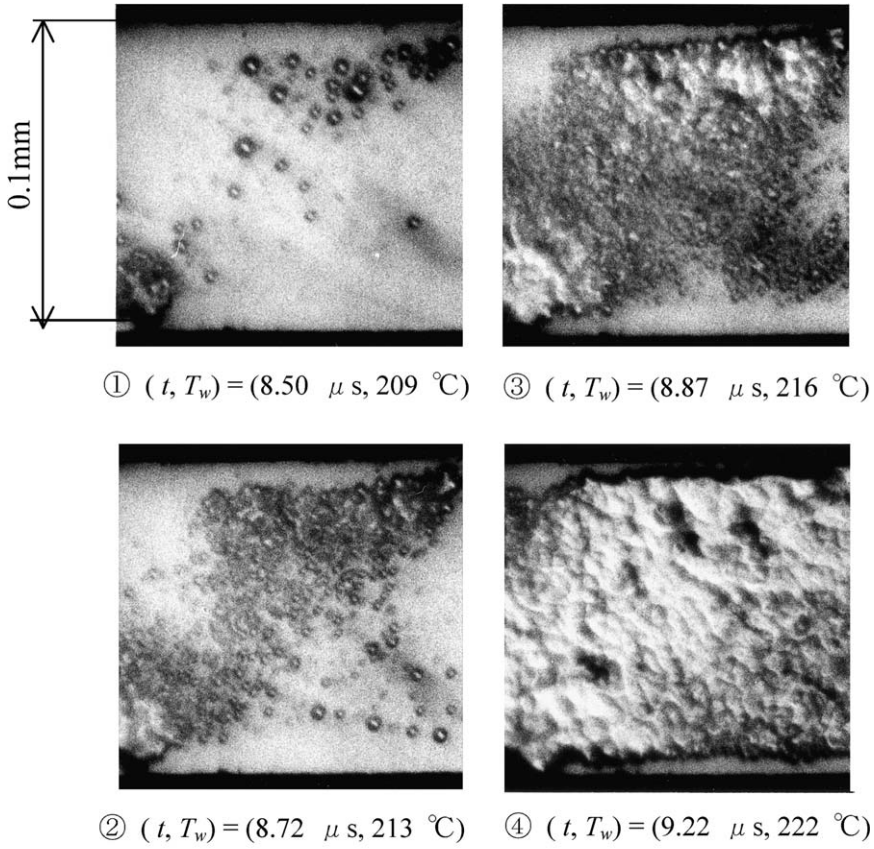

Fig. 4(b). Magnified top view of boiling bubbles immediately after boiling incipience on the film heater subjected to high pulse heating (ethyl alcohol, $P = 0.1$ MPa, $T_{l0} = 25$ °C, $\overline{B} = 2.2 \times 10^7$ K/s).

regardless of the magnitude of the heating rate for a sufficiently large rate. The small superheat energy may result in the small growth and rapid collapse of the vapor bubble. The boiling features presented in Figs. 4–6 provide evidence that supports this conclusion.

4. Analysis of bubble growth by evaporation of the superheated liquid layer

Based on the results shown in the preceding section, rather than the dynamics of each nucleated bubble, the dynamics of the coalesced bubble succeeding spontaneous nucleation are found to be significant with respect to vapor generation and/or the volumetric expansion. As the heating rate is increased, the coalesced bubble became a thin vapor film that grew uniformly over the heater. The coalesced bubble may have grown by the vapor mass production due to self-evaporation from the highly superheated liquid layer that developed before the boiling incipience as well as the acceleration of the liquid pushed away by the vapor pressure.

In the present section, the dynamic growth of the coalesced bubble due to the evaporation of the superheated liquid layer and the subsequent collapse are analyzed using the theoretical model shown in Fig. 7.

The following assumptions were made:

(1) As soon as spontaneous nucleation occurs over the entire heater surface that is rapidly heated up to the homogeneous nucleation temperature, a thin vapor film is formed by the coalescence of the generated bubbles. The initial temperature and the initial pressure of the vapor film are equal to the spontaneous nucleation temperature and the corresponding saturation vapor pressure, respectively.
(2) The vapor film thickness grows uniformly due to the self-evaporation of the superheated liquid layer that forms on the heater surface before boiling incipience. The heat capacity of the vapor and the heat transfer through the vapor film are neglected.
(3) The evaporation (or condensation) rate is determined by the heat flux at the vapor–liquid interface, which can be estimated by assuming the one-dimensional transient heat conduction in the liquid.
(4) The temperature at the vapor–liquid interface is always equal to the saturation temperature corresponding to the vapor pressure, which varies with time according to the liquid motion while being uniform in the vapor film.

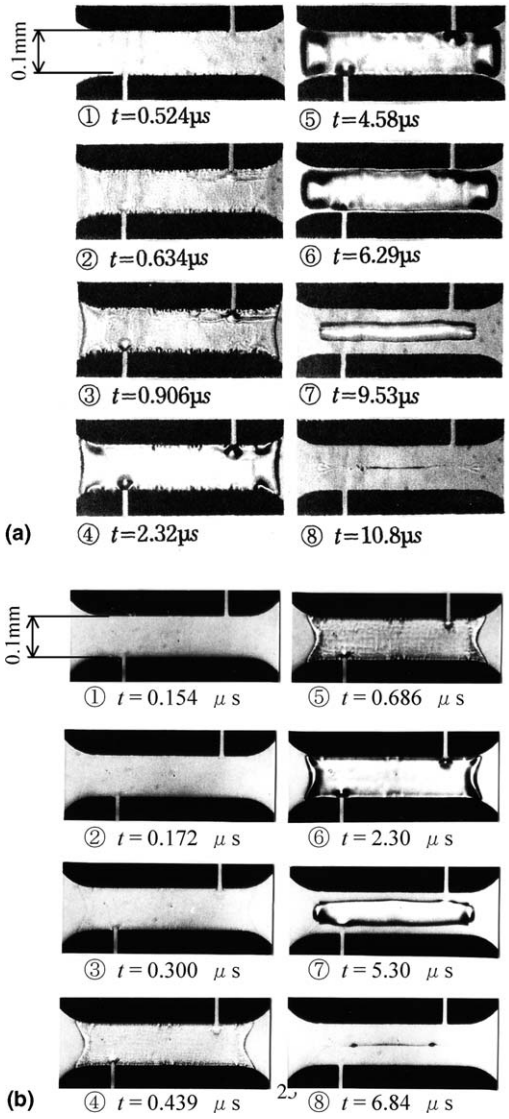

Fig. 5. Boiling configurations after boiling incipience on the film heater at high heating rates (ethyl alcohol, $P = 0.1$ MPa, $T_{l0} = 25$ °C): (a) $(\overline{B} = 3.7 \times 10^8$ K/s)*, $(q_{lBI} \cong 300$ MW/m$^2)$*, $\tau_h = 1$ μs, (b) $(\overline{B} = 1.2 \times 10^9$ K/s)*, $(q_{lBI} \cong 900$ MW/m$^2)$*, $\tau_h = 0.2$ μs.

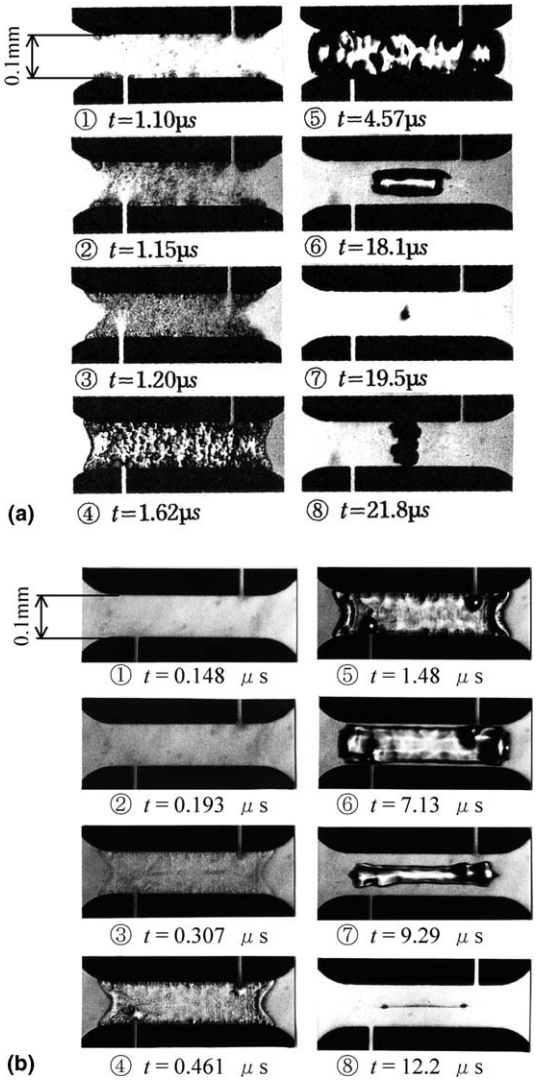

Fig. 6. Boiling configurations after boiling incipience on the film heater at higher heating rates (water, $P = 0.1$ MPa, $T_{l0} = 25$ °C): (a) $(\overline{B} = 2.6 \times 10^8$ K/s)*, $\tau_h = 1.1$ μs, (b) $(\overline{B} = 1.8 \times 10^9$ K/s)*, $\tau_h = 0.2$ μs.

(5) The liquid motion on the heater is equal to that in a semi-infinite liquid region on a flat wall to which the heater is attached. The effects of liquid compressibility and surface tension are neglected.
(6) The vapor behaves as an ideal gas.

Under these assumptions, the equation of motion is expressed as

$$A_l \frac{d^2 V_v}{dt_g^2} = P_v - P_\infty \tag{2}$$

where V_v $(= \delta_v S_h)$ is the volume of the vapor film, δ_v the thickness of the vapor film, S_h the heater surface area, P_v the pressure in the vapor film, P_∞ the ambient pressure, and A_l the inertance of the liquid region surrounding the heater, which is approximated as $A_l \approx 0.43\rho_l/d_h$ for a square having sides of length d_h located on a flat wall facing a semi-infinite liquid [7].

The mass conservation equation for the vapor film is given by

$$\frac{d(\rho_v V_v)}{dt_g} = \frac{q_i S_h}{H_{fg}} \tag{3}$$

where q_i is the heat flux at the vapor–liquid interface.

Based on the heat conduction theory [15], the heat flux at the vapor–liquid interface on the liquid side can be expressed as

$$q_i = \frac{\lambda_l}{\sqrt{\pi\kappa_l}} \left(- \int_0^{t_g} \frac{\partial T_i}{\partial \tau} \frac{d\tau}{\sqrt{t_g - \tau}} \right) - q_{lBI} \tag{4}$$

where T_i is the temperature at the vapor–liquid interface and equal to the saturation temperature corresponding to P_v, q_{lBI} the wall heat flux from the heater surface to the liquid immediately before the boiling incipience, which

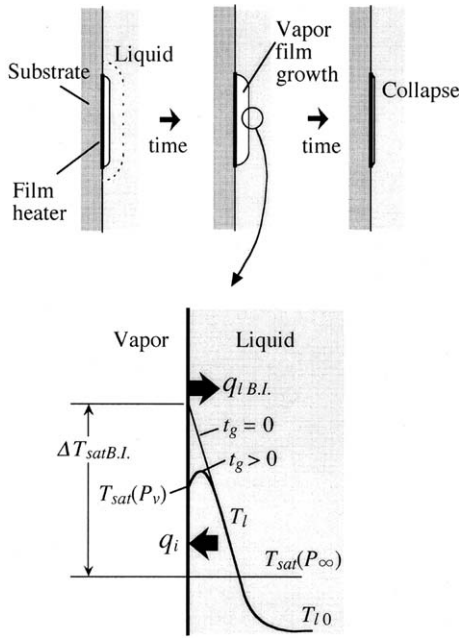

Fig. 7. Model for dynamic growth of the coalesced bubble due to evaporation of the superheated liquid layer and subsequent collapse.

increases with the rate of the wall temperature increase. Here, q_{lBI} was approximated not to change during the vapor film growth and collapse.

Eqs. (2)–(4) were solved simultaneously under the following initial conditions, and the numerical solutions of V_{v} and P_{v} were obtained:

$$\frac{\mathrm{d}V_{\mathrm{v}}}{\mathrm{d}t_{\mathrm{g}}} = 0 \quad \text{and} \quad V_{\mathrm{v}} = V_0\ (= \delta_{\mathrm{v0}} S_{\mathrm{h}}) \quad \text{for } t_{\mathrm{g}} = 0 \tag{5}$$

where, as the initial volume of the vapor film V_0, a sufficiently small and non-zero value that does not affect the subsequent growth was assumed.

Fig. 8 show the calculated time-variations of the vapor film thickness, the vapor pressure and the growth rate of the vapor film thickness, respectively. In these figures, q_{lBI} was changed as the parameter. The corresponding rate of temperature increase can be expressed approximately as

$$\overline{B}\ (\mathrm{K/s}) = 1.3 \times 10^6\ (q_{\mathrm{lBI}}(\mathrm{MW/m^2}) - 12) \tag{6}$$

for $1.0 \times 10^7 \leqslant \overline{B} \leqslant 1.7 \times 10^8$ (K/s), based on the experimental results for ethyl alcohol obtained in the present study. The calculated vapor film thickness increases with time up to the maximum value before decreasing. The maximum thickness decreases with the increase in q_{lBI}, because the stored superheat energy before the boiling incipience is smaller at the larger q_{lBI}. This tendency of the maximum thickness on the heating rate agrees qualitatively with the observed results shown in Figs. 4 and 5. The measured thicknesses (in the central region of the heater) and growth rates of the bubbles shown in Fig. 4(a) are also plotted in the Fig. 8(a) and (c), respectively. The value of q_{lBI} at the heating rate shown in Fig. 4(a) was 35 MW/m^2. The overall tendencies of the time-variations of the vapor film thickness and the growth rate, as well as the maximum values, are consistent with the experimental results. The compressibility of the liquid, if taken into account, may cause only a

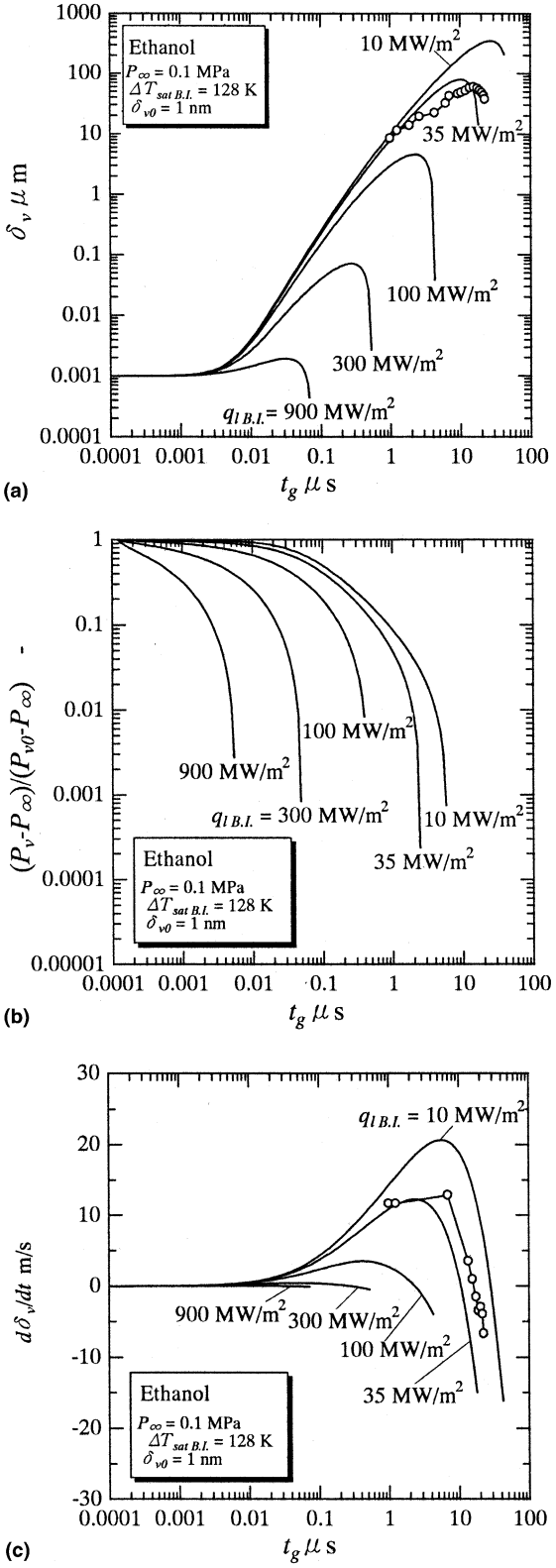

Fig. 8. Calculated time variations of (a) vapor film thickness, (b) pressure in vapor film and (c) vapor film growth rate.

slight deviation, less than approximately 1 μm, in the estimation of the vapor film thickness. In Fig. 8(b), the vapor pressure is shown as the excess pressure beyond the ambient pressure ($P_v - P_\infty$) normalized by the initial value. In the case of $q_{lBI} = 35\ MW/m^2$, the excess pressure significantly decreases to less than 1% of the initial value only a few microseconds after the onset of the growth and then becomes negative. After the vapor pressure (absolute value) decreases to be much lower than the ambient pressure, the vapor film grows considerably. Therefore, the inertia of the liquid that is accelerated by the vapor pressure, as well as the evaporation from the superheated liquid, may also have a considerable effect on the growth of the vapor film.

Fig. 9 compares the measured and calculated growth periods up to the maximum size τ_g. The calculated periods are of nearly the same order as the measured ones for the heating rates smaller than 1.7×10^8 (K/s) which is the maximum rate that the heater temperature can be measured without the loss of accuracy, although the dependence on the heating rate is somewhat different. The disagreement at lower heating rates may be due to the multi-dimensional effect during the actual growth, because the vapor layer grows in a round shape as shown in Fig. 4(a). At higher heating rates, the measured growth periods tend to become larger than the calculated ones. As described above, the thicker vapor film regions are observed around both heater ends at higher heating rates (Figs. 5(a), (b) and 6(b)). The reduced heating rate due to the enlarged width around the end regions may result in the larger superheat energy storage, and therefore, larger (or thicker) and delayed growth, as can be seen in Fig. 8(a). The inflow of vapor from the end regions to the central region may cause the significant delay in the collapse of the thin vapor film in the central region. Such end effect may be the reason of the larger measured period compared to the calculated results. The delayed growth around the end regions also seems to affect the collapse behavior of the entire vapor film.

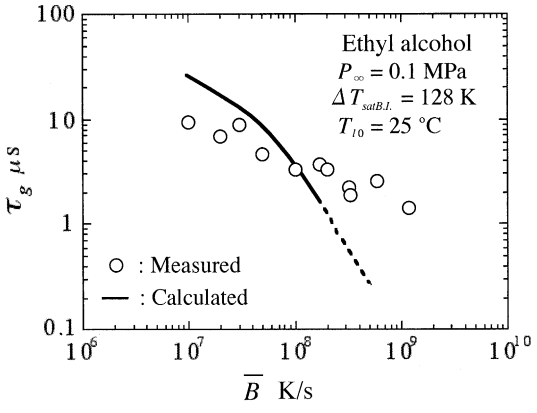

Fig. 9. Measured and calculated growth periods of vapor film as a function of the rate of temperature rise.

5. Conclusions

The dynamics of boiling succeeding spontaneous nucleation on a small film heater immersed in ethyl alcohol were investigated under heating conditions such that the inception of boiling is dominated by spontaneous nucleation. The heating rate was widely varied from the minimum rate required for realizing spontaneous nucleation up to a rate of approximately two orders of magnitude larger than the minimum rate.

The following conclusions were obtained:

(1) A large number of tiny bubbles generated concurrently due to spontaneous nucleation coalesce with each other to form a vapor film, which grows into a single bubble that covers the entire heated surface. As the heating rate is increased, individual nucleated bubbles become difficult to distinguish and a very thin vapor film appears to form uniformly over the heated surface. The vapor film does not grow significantly to form a massive bubble, and only a thin film collapses. Similar behavior was also observed for water.

(2) A theoretical model of the dynamic bubble growth due to self-evaporation of the superheated liquid layer that develops before boiling incipience was presented. The calculated time-variation of the vapor film thickness and its dependence on the heating rate agreed qualitatively with the experimental results.

References

[1] Y. Iida, K. Okuyama, K. Sakurai, Peculiar bubble generation on a film heater submerged in ethyl alcohol and imposed a high heating rate over 10^7 K/s, Int. J. Heat Mass Transfer 36 (10) (1993) 2699–2701.

[2] Y. Iida, K. Okuyama, K. Sakurai, Boiling nucleation on a very small film heater subjected to extremely rapid heating, Int. J. Heat Mass Transfer 37 (17) (1994) 2771–2780.

[3] Y. Iida, K. Okuyama, T. Endou, N. Kanda, Boiling nucleation on a very small film heater subjected to extremely rapid heating (effect of ambient pressure on bubble formation by fluctuation nucleation), JSME Int. J., Ser. B 40 (2) (1997) 250–256.

[4] Y. Iida, K. Okuyama, T. Nishizawa, Heat transfer during boiling initiated by fluctuation nucleation on a platinum film rapidly heated to the limit of liquid superheat (1st report, experiment under atmospheric pressure condition), Trans. JSME, Ser. B 63 (613) (1997) 3048–3054.

[5] K. Okuyama, Y. Iida, Boiling bubble behavior and heat transfer succeeding spontaneous nucleation on a film heater, in: Proceedings of 11th International Heat Transfer Conference, vol. 2, 1998, pp. 527–532.

[6] A. Asai, S. Hirasawa, I. Endo, Bubble generation mechanism in the bubble jet recording process, J. Imaging Technol. 14 (5) (1988) 120–124.

[7] A. Asai, Bubble dynamics in boiling under high heat flux pulse heating, J. Heat Transfer 113 (1991) 973–979.

[8] I. Ueno, M. Shoji, Experimental study of nucleation and pressure generation induced by nanosecond laser pulse heating of metal in water, in: Proceedings of the 5th ASME/JSME Thermal Engineering Joint Conference, 1999, pp. 1166–1174.

[9] Z. Zhao, S. Glod, D. Poulikakos, Pressure and power generation during explosive vaporization on a thin-film microheater, Int. J. Heat Mass Transfer 43 (2000) 281–296.
[10] C.T. Avedisian, W.S. Osborne, F.D. McLeod, C.M. Curley, Measuring bubble nucleation temperature on the surface of a rapidly heated thermal ink-jet heater immersed in a pool of water, Proc. Roy. Soc. London, A 455 (1999) 3875–3899.
[11] M. Volmer, Kinetics der Phasenbildung, Steinkopff, 1939.
[12] V.P. Skripov, Metastable Liquids, John Wiley, New York, 1974.
[13] M.G. Cooper, A.J.P. Lloyd, The microlayer in nucleate pool boiling, Int. J. Heat Mass Transfer 12 (1969) 895–913.
[14] K. Okuyama, S. Tsukahara, N. Morita, Y. Iida, Transient behavior of boiling bubbles generated on the small heater of a thermal ink jet printhead, Exp. Therm. Fluid Sci. 28 (2004) 825–834.
[15] H.S. Carslaw, J.C. Jaeger, Conduction of Heat in Solids, second ed., Oxford University Press, London, 1959, p. 62.